

A Search for Stellar Obscuration Events due to Dark Clouds

A. J. Drake^{1,2,3}, K. H. Cook¹

ABSTRACT

The recent detections of a large population of faint submillimetre sources, an excess halo γ -ray background, and the extreme scattering events observed for extragalactic radio sources have been explained as being due to baryonic dark matter in the form of small, dark, gas clouds. In this paper we present the results of a search for the transient stellar obscurations such clouds are expected to cause. We examine the Macho project light curves of 48×10^6 stars toward the Galactic bulge, LMC and SMC for the presence of dark cloud extinction events. We find no evidence for the existence of a population of dark gas clouds with $A_V > 0.2$ and masses between $\sim 10^{-4}$ and $10^{-2}M_\odot$ in the Galactic disk or halo. However, it is possible that such dark cloud populations could exist if they are clustered in regions away from the observed lines of sight.

Subject headings: ISM: clouds – dust, extinction – Galaxy : halo – dark matter

arXiv:astro-ph/0301013v1 1 Jan 2003

¹Lawrence Livermore National Laboratory, 7000 East Ave, Livermore, CA 94550

²Dept. of Astrophysical Sciences, Princeton University, Princeton, NJ 08544

³Depto. de Astronomia, P. Universidad Catolica, Casilla 104, Santiago 22, Chile

1. INTRODUCTION

It has been proposed that a large fraction of the baryonic dark matter in the halo of our Galaxy could be in the form of cold, dense gas clouds (de Paolis et al. 1995, Gerhard & Silk 1996). Such clouds would be extremely difficult to detect directly with traditional means due to their dark nature. However, the extreme scattering events observed by Fiedler (1987) have been given as evidence for AU-sized, planetary-mass gas clouds (Henriksen & Widrow 1995, Walker & Wardle 1998). Further evidence for the existence of such clouds comes from the detections of large populations of faint sub-mm sources detected by SCUBA (Submillimetre Common User Bolometric Array) (Lawrence 2001). Yet more evidence for such a population comes from recent EGRET (Energetic Gamma Ray Explorer Telescope) results which show the presence of a background γ -ray emission from the Galactic halo. Kalberla, Schekinov and Dettmar (1999) have suggested that these results can be explained as due to the interaction of high energy cosmic rays with dense H_2 clumps with masses $\sim 10^{-3}M_\odot$ and radii ~ 6 AU. These detections and prior observational and dynamical arguments have lead to further suggestions about how a halo dark cloud population could be discovered (Kerins, Binney & Silk 2002, hereafter KBS; Kamaya and Silk 2002). Although most models place the cloud population within the halo, Pfenniger and Combes (1994) suggested that such clouds are a natural part of the cold ISM and would exist concomitant with the thin HI disk.

For dark clouds to have survived until the present day, they must have a mass which is sustainable over a Hubble time. Within the Galaxy the lower mass limit is $10^{-6}M_\odot$ because smaller masses will evaporate due to cosmic ray heating (Wardle & Walker 1999). It is also expected that these objects will contain some metals since it has been suggested that clouds with primordial composition can not cool below 100K (Murray &

Lin 1990). Any population of gas clouds must be much cooler than this to have escaped detection in previous surveys (Lawrence 2001). The presence of a small amount of metals can assist the cooling of gas clouds (Gerhard & Silk 1996). It has been suggested that, even if the clouds were dust-free, they could be stabilized against gravitational collapse by cosmic ray heating (Sciama 2000). However, if the SCUBA sources are due to clouds they must contain some dust to exhibit continuous emission in the sub-mm band (Lawrence 2001). The SCUBA results led to likely cloud masses of $10^{-4} - 2 \times 10^{-2}M_\odot$ with temperatures < 18 K. The virial radius of a cloud with $T = 18$ K and $M = 10^{-4}M_\odot$ is 0.39AU, and for a cloud with $T = 10$ K and $M = 10^{-2}M_\odot$ the virial radius is 70AU. These radii set likely-limits on the sizes of a gas cloud population. Further limits on clouds sizes and masses come from constraints on gaseous lensing events. Raficov and Draine (2001) note that no gaseous lensing events have been observed toward the LMC by the MACHO project, while many events are expected for a significant population of compact gas clouds. Massive compact objects such as clouds, stars, or other objects will lense stars as they pass through our line-of-sight of the stars. Since lensing is not observed any clouds present must exceed the projected Einstein radius. The analysis of Raficov and Draine (2001) suggests that cloud must have radii from 2 to 300AU, for cloud masses between $M = 10^{-4}$ and $2 \times 10^{-2}M_\odot$ for temperatures of 10 to 100K. Another constraint on the dark clouds comes from the EGRET results of Kalberla et al. (1999). They find that the γ -ray results are consistent with H_2 clumps with masses $0.3 - 3 \times 10^{-3}M_\odot$ and sizes from 3 to 10AU.

One consequence of the existence of a population of small dark clouds is the transient obscuration of background stars (Gerhard & Silk 1996). Such events are expected to be very rare with much less than 1% of stars in any given direction being obscured at any time. However,

even a very low rate of obscuration events is detectable with the data from microlensing experiments, since millions of stars have been observed for many years (Alcock et al. 2000; Udalski et al. 2000; Derue et al. 2001; Bond et al. 2002). Models for the obscuration event timescale distribution of cloud occultation events have been presented by KBS. They consider two hypothetical cloud populations, one in which the clouds occupy the disk and another where they reside in the Halo.

In this paper we present the results of an analysis of the MACHO light curve dataset to detect light curves consistent with extinction due to passing dark clouds. We will search for events toward stars in the disk (Galactic bulge) and the Halo (LMC and SMC). To quantify our results we determine our detection efficiency for the various possible dark cloud parameters in the KBS models.

2. OBSERVATIONS

The MACHO project repeatedly imaged ~ 67 million stars in a total of 182 observation fields toward the Galactic bulge, the LMC and SMC, to detect the phenomenon of microlensing (Alcock et al. 1997). The data was taken in $\sim 90,000$ individual observations, each covering a total area of $43' \times 43'$ on the sky. When field overlap is considered, the 182 fields observed cover approximately 80 square degrees. These images were taken between 1992 and 2000 on the Mount Stromlo and Siding Springs Observatories' 1.3M Great Melbourne Telescope with the 8×2048^2 pixel dual-colour wide-field *Macho camera*. Observations toward the Galactic bulge have exposure times of 150 seconds while toward the LMC and SMC they have 300 and 600 seconds, respectively. The photometry was carried out using a fixed position PSF photometry package derivative of the DoPhot package (Schechter, Mateo & Saha 1993) called SoDOPHOT (Bennett 1993). The images were taken with non-standard B_M and R_M bands and can be converted to the stan-

dard Kron-Cousins system V and R using the photometric calibrations are given in Alcock et al. (1999). The dataset provides a consistent set of photometry for stars spanning the duration of the experiment.

The observations toward the LMC and the SMC were taken all year round, while the Galactic bulge was observed between March and October. The median seeing of the data set is roughly $2''$ and measurements reach stars with V -band magnitudes between 21 and 22. The photometric sampling frequency varies greatly between the individual fields observed toward the Galactic bulge and the LMC. The least sampled fields have only ~ 50 observations while those most sampled have ~ 2000 observations. For most fields, observations are quite evenly spaced over the experiments duration (apart from the observing gaps toward bulge fields). However, a few fields in the LMC and the Galactic bulge have variations in observation frequency because of changes in the observing strategy. Also, a small number of the bulge fields were only observed in the last few years of the project.

To select candidate obscuration events from the MACHO database we performed a number of cuts to remove data which was noisy or had a low signal-to-noise ratio. We selected stars with magnitudes between $13 < V < 21$ toward the Galactic bulge and LMC and $14 < V < 22$ for the SMC. For each of the stars in this range we determined the median magnitude, M_{10} , and the standard deviation, σ_{10} , based on the first 10% of the data points. However, if there were less than 500 observations in a light curve we used the first 50 data points. We rejected any light curves where σ_{10} was larger than 0.7 magnitudes in either passband. Altogether these cuts removed $\sim 40\%$ of the stars observed. The parameters of the analyzed dataset are given in Table 1.

3. SEARCHING FOR OBSCURATION EVENTS

In this analysis we aimed to detect stellar occultations due to opaque dust clouds and obscurations due to dark clouds with a small dust-to-gas ratio. We also tried to detect gas cloud transits without restricting the cloud shapes to purely spherical morphology or isotropic dust distribution. Therefore, to find events due to the passage of dark clouds in front of stars, we were as liberal as possible in our selection of the light curves which might exhibit extinction effects.

Firstly, we selected light curves that exhibited a significant drop in flux that lasted > 10 days. This selection was required to remove eclipsing binaries and data that was affected by periods of bad observing conditions. Secondly, we required that the photometry points during the candidate obscuration event were > 0.2 magnitudes below the median magnitude and had $> 4\sigma$ significance. The uncertainty, σ , was based on the distribution of the photometry values rather than the individual photometric uncertainties. As the detection of candidate obscuration events is sensitive to the sampling rate of a target field, we also required at least 10 points below the median in any candidate event. To reduce the number of long period variables detected, we only accepted light curves with $< 50\%$ of the points below M_{10} , (the 10% median value). However, we did not require that the flux in a candidate's light curve returned to the median value. In this way, we hoped to retain some of the sensitivity to dark cloud extinction events with timescales longer than the Macho projects baseline (~ 8 yrs).

Applying these criteria to the MACHO project photometry data, 5284 ($\sim 0.016\%$) light curves passed our initial selection toward the Galactic bulge, 6427 ($\sim 0.050\%$) toward the LMC and 678 ($\sim 0.027\%$) toward the SMC. From examination of the candidate's light curves and their positions in CMDs, it was clear that most of the objects passing these selections were long period variables. This was to be expected since these stars

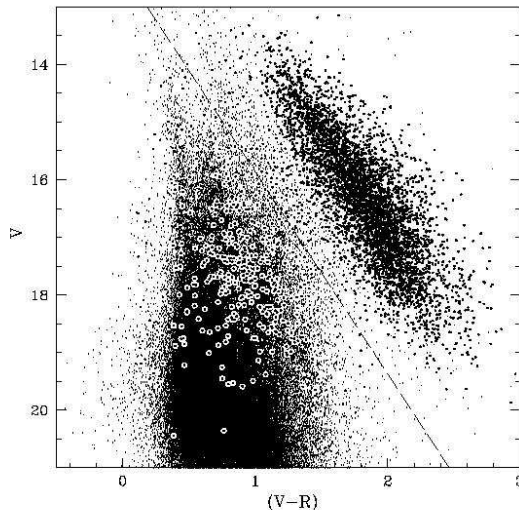


Fig. 1.— The initial obscuration event candidates selected from all Galactic bulge light curves. Stars toward the bulge fields are represented by small dots while candidates are represented by larger ringed-dots. The dashed-line shows the selection criteria used to remove variables from our lists.

have large variability amplitudes, timescales $\gtrsim 80$ days, and red colours. However, we intended to examine the light curves before applying any colour selection criteria which might bias our results. As none of the light curves in the AGB region of the CMD appeared consistent with dark cloud transit events, we chose to apply empirical colour selections to the candidates toward each target direction. In Figures 1 and 2 we present CMDs of the Galactic bulge, LMC and SMC stars. The CMDs are composed of a ~ 1000 stars from each of the 182 fields observed. In each figure we have over-plotted the M_{10} magnitudes of the light curves passing our primary selection as obscuration events. We have also plotted the colour cuts we applied to remove the AGB variables (to the right of the dashed-line) which passed our initial selection criteria. As can be clearly seen, this colour selection removes al-

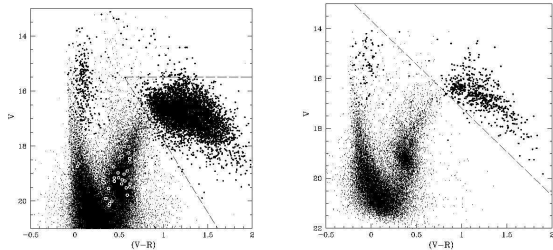


Fig. 2.— LMC and SMC dark cloud obscuration event candidates. Left panel: the median magnitudes for candidate light curves toward the LMC. Right panel: same as the left, but for candidates toward the SMC. The small dots are normal stars within the Magellanic cloud fields and larger ringed-dots are the candidates. The candidates to the right of the dashed-line are deemed to be due to normal stellar variability.

most all the initial candidates. However, these colour cuts only remove $\sim 1\%$ of all stars toward any of the target fields, so they do not significantly change our total exposure. After applying the red variable star cuts there were 372, 441 and 98 remaining candidates toward the Galactic bulge, LMC and SMC, respectively. Many of these objects were also clearly variable stars.

Toward the Galactic bulge many of the candidate events had clump star sources. Almost all of these light curves exhibit sinusoidal modulations superimposed on a varying baseline magnitude. The oscillation periods were found to be between 11 and 90 days with amplitudes between 0.02 and 0.2 magnitudes. These stars exhibited baseline magnitude changes of up to ~ 0.5 magnitudes. All these features are typical of chromospherically-active stars (Fekel, Henry, & Eaton 2002) and can not be explained simply by a transiting dark cloud. Of the candidate events 155, 10, and 2 light curves (Galactic bulge, LMC, SMC) were clearly due to chromospherically-active stars and were removed. The variation in the number of objects toward the target fields is due to stellar populations differences and to the

fact that the photometry of clump stars is poorer at the distances of Magellanic cloud stars.

A large number of the candidates in the Magellanic cloud fields were found to be due to the well known population of bright, blue, *Be* variable stars known as bumpers (Keller et al. 2002). These stars occupy a restricted region of the CMD and can show long dips similar to those expected for a cloud transit. However, many also exhibit outbursts similar to dwarf novae. Such flares are not easily explainable in a cloud transit model. We removed an additional 89, 280, and 55 (Galactic bulge, LMC, SMC) exhibit either obvious flares or multiple dips below the baseline magnitude. Although it is possible that a star could be eclipsed by more than one cloud within a period of a few years, this seems extremely unlikely given the the small number of candidates relative to the total number of stars analyzed.

Of the candidate cloud transit events 45, 18 and 1 (Galactic bulge, LMC, SMC) were discovered to be due to high proper motion stars. These objects have very characteristic light curves shapes. In such curves the dip in magnitude is actually due to the movement of the star away from the fixed position where photometry is performed (Alcock et al. 2001). These light curves show increased scatter with time and never return to the baseline flux level. In our selection process we only removed the light curves which exhibited increasing scatter with time to a degree significantly larger than expected for stars of their measured magnitudes. After removing the variable stars, etc, 83 Galactic bulge, 133 LMC, and 36 SMC candidates remained.

If the dips observed in candidate’s light curves are due to extinction caused by dusty clouds, the obscured stars should become redder as they fade along the extinction vector. The exact amount of reddening should depend on the quantity and nature of the dust present. To test this scenario, we assumed that the detected drop in flux was purely due to dust extinction. In this case the magnitude during an obscuration event should

be well represented by,

$$V = C + R_{VR}\Delta(V - R), \quad (1)$$

where C is the baseline flux, $\Delta(V - R)$ is the change in the star's colour and $R_{VR} = A_V/E(V - R)$ is the ratio of total to selective extinction for the bands we observed. The V -band light curve of each candidate was fitted to determine the value of R_{VR} .

We expect that, if the drop in flux was only due to varying amounts of dust (producing varying degrees of extinction), the reduced χ^2 of this fit should be close to 1. However, if the drop in flux is caused by variability which is not consistent in the two passbands the fit will be poor. Furthermore, if the dust composition within a cloud follows standard dust properties, the value of the extinction should be similar to that expected for standard reddening law $R_V = A_V/E(B - V) = 3.1$ (Cardelli, Clayton, & Mathis 1989). However, there is some evidence for variations from the standard extinction law toward the Galactic bulge. For example, Udalski (2002) found R_V values between 1.8 and 3.3 in the extinction ratio for Galactic bulge fields. Low R_V values have also been observed by Szomoru & Guhathakurta (1999), whom found $R_V \lesssim 2$ for a sample of Galactic cirrus clouds. However, Clayton & Cardelli (1988) reported that extinction values are typically between 2.6 and 5.5. The observed differences in R_V from the standard value have been attributed to variations in silicate and graphite grain size distributions (Kim, Martin, & Hendry 1994, Larson et al. 2000). To be comprehensive in our candidate event selection, we selected light curves having fit coefficients corresponding to R_V between 1.8 and 5.5. Using the relative extinction for our passbands from by Schlegel, Finkbeiner, & Davis (1998) we transform our results from R_{VR} to R_V . We adopted the same R_V limits for the candidate light curves toward all targets.

The reduced χ^2 fit value is sensitive to how

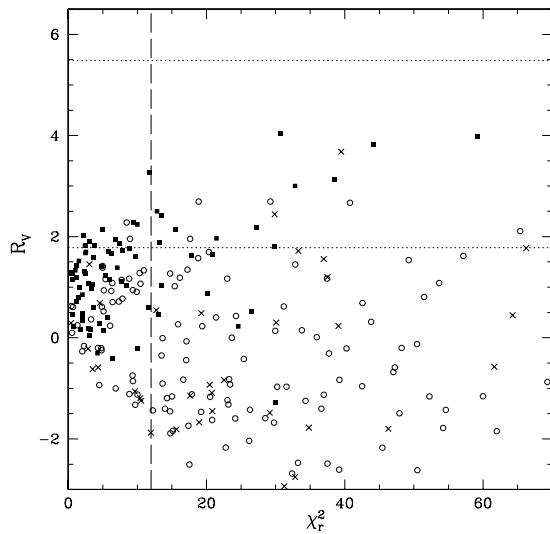


Fig. 3.— Reddening fit values for candidate cloud obscuration events. The dotted line show the expected limits if the dips on the light curves are due to dust reddening. The dashed line shows maximum χ_r^2 expected for the fit in the presence of underestimated errors and varying dust composition along the line-of-sight through a cloud. The filled squares show Galactic bulge candidate fits, while the circles and crosses present results for LMC and SMC candidates, respectively.

well the magnitude uncertainties are determined and whether the dust composition varies within a cloud. The flux measurement uncertainties are highly unlikely to be incorrect by more than a factor of 3. The degree of variation in the dust composition within a cloud is completely unknown, but it seems unlikely to be large. Most of the light curves are well sampled with a few hundred data points. Therefore, it seems unlikely that a χ_r^2 value greater than 12 could occur even with poorly estimated photometric uncertainties and varying dust composition within a cloud. In Figure 3 we plot the values of R_{VR} for the MACHO V -band light curves against the reduced χ^2 values of the fit.

Of the remaining candidates, 10 bulge, 2 LMC

and 0 SMC light curves passed our extinction criteria. In Table 2 we present the number of candidate obscuration events remaining after each selection criterion was applied. From examination of their light curves it seems likely that most, if not all, of these light curves are due to variability rather than extinction effects. Furthermore, they do not appear to be near the location representative of the most common stars. This suggests that they are simply outliers among the thousands of variable stars present in the fields.

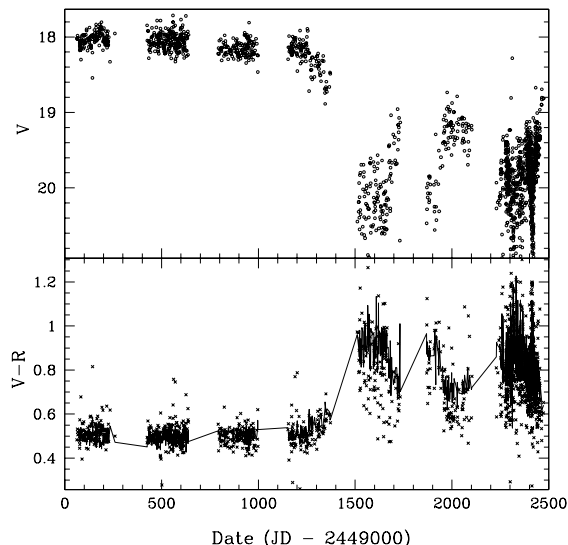


Fig. 4.— The light curve for the best dark cloud transit candidate (MACHO object ID 119.20740.1031). In the upper panel we present the V-band light curve and in the lower panel the colour curve. Over-plotted on the lower panel is the fitted colour coefficient for this light curve.

In Figure 4 we present the light and colour curves for the Galactic bulge candidate which appears the most like that expected for a cloud transit event. In this case, the object gets redder when it fades as expected for a cloud transit. For the standard reddening law ($R_V = 3.1$), we expect to measure $R_{V_R} = 5.2$ in our filters. The fit of the light curve of this candidate gives $R_{V_R} = 5.1 \pm 0.1$. Although the agreement is very

good, the photometry of the faint data points is very uncertain. Almost all of the other candidate’s light curves exhibit drops < 1 magnitude. However, the Galactic bulge light curve with MACHO ID number 120.21786.958 has a drop > 3.5 magnitudes and is also a good candidate obscuration event. If any of the the other candidates were due to dark cloud events they would have to have a very small dust-to-gas ratio compared to molecular clouds. The lack of a significant number of obscuration event detections is significant, but must be quantified to provide a useful limit on cloud models.

4. DETECTION EFFICIENCIES

To determine the significance of our result it is necessary to know how the selections we have made will affect our efficiency of detection. Any obscuration event will have a start time, a timescale, a maximum extinction, and an impact parameter. The expected occultation timescale distribution for virialized dark clouds with $T = 10\text{K}$ and $R = 7\text{AU}$ in fields toward the Galactic bulge, LMC, and SMC, is given by KBS. The KBS models consider two possible dark cloud populations, a halo one and a disk one. The halo model consists of clouds in an isothermal halo with a core radius of 5 kpc, a local density of $0.01\text{M}_\odot\text{pc}^{-3}$ and a Gaussian velocity dispersion of 156km s^{-1} . The disk model consists of a sech-squared disk with scale-length 2.5 kpc, scale height 190pc and density $0.03\text{M}_\odot\text{pc}^{-3}$. Here the Galactic rotational velocity of the clouds and stars is taken to be 220km s^{-1} with 25km s^{-1} dispersion. Although our analysis should be sensitive to a broader range of possible cloud parameters than those of KBS, their models are well constrained. Therefore, we will determine how efficiently dark clouds following the KBS models would have been detected in our analysis. For simplicity, we assumed that the dust was isotropically distributed within each cloud and that the obscuring clouds should not exhibit any preference in their alignment with

background stars. We have, therefore, selected cloud-star obscuration impact parameters from a uniform distribution between 0 and 1 cloud radii. To determine our sensitivity to varying amounts of dust we assumed a uniform distribution of the dust-to-gas fraction relative to Galactic molecular clouds, f , to be between 0 and 0.1. This ratio corresponds to a visual extinctions between 0 and 12 magnitudes (Binney & Merrifield 1998). For our analysis, an extinction of 12 magnitudes corresponds to the opaque cloud limit since even the brightest stars in our fields would become undetectable.

For us to have detected any occultation events within our analysis it would have to either start or finish within the observing period of the MA-CHO project. Therefore, we produced a randomly distributed set of artificial extinction events lying within the observational time frame. For each of the Galactic bulge, LMC and SMC datasets we produced ~ 10 million artificial events. Many events were added to the same light curves in one dataset (corresponding to a $2' \times 2'$ region) for each of the 182 fields we analyzed. Each of these datasets typically contain the photometry for a few thousand stars. Although this is only a small fraction of the stars within a field, we believe this number was sufficient to represent the overall properties of a field since the observational properties will be the same throughout a field. As there were less than 10 million stars chosen toward each target, we added a number of artificial obscuration events to each light curve. These extinction events were added to both red and blue Macho light curves. The observed drop in flux for each light curve was calculated from the optical depth through the cloud at the cloud-star impact parameter. The extinction was taken to follow the standard reddening law ($R_V = 3.1$). Light curves with the artificial cloud obscuration events were processed through the same selections as the real data up until the point where we removed the chromospherically active stars. At this point there were a few hundred objects

found toward each target in our survey. We have not attempted to parameterize and implement the additional selections here since this would be a very complex and somewhat contrived process. However, we believe the selections we made to remove the variable stars, etc, were fairly robust and would have little effect on our calculated detection efficiency.

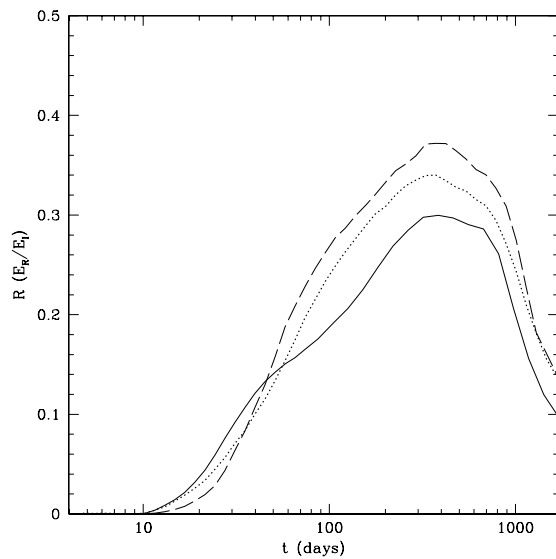


Fig. 5.— Number of recovered events R as a function of their input obscuration event timescales. Solid-lines show obscuration events detection efficiencies toward Galactic bulge fields, dotted-line, toward LMC fields, dashed-line, toward SMC fields.

In Figure 5 we show the distribution of artificial obscuration events recovered for the Galactic bulge, LMC and SMC. For all targets the peak detection efficiency is around 350 days. In general, as the timescale of the obscuration events increases, the signal-to noise ratio of even a small drop in flux increases. However, at longer timescales the events are more likely to be occurring at the beginning of the light curve where the baseline is determined. Therefore, no dip is measured relative to the median magnitude. At very long timescales such clouds are more likely to be

transiting throughout the observation time. Almost all obscuration events lasting less than ten days are not detected because of the minimum timescale cut we imposed.

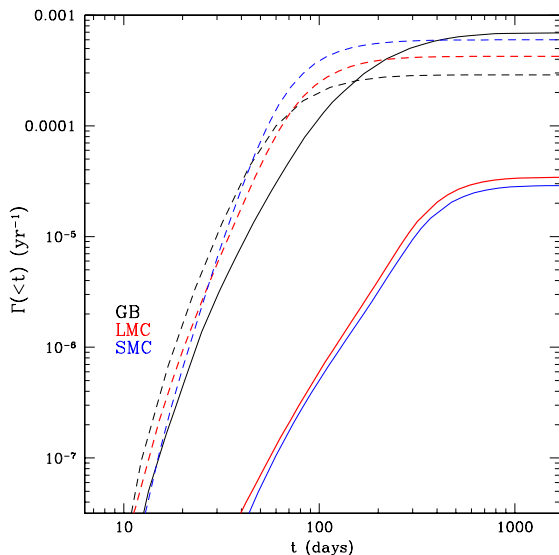


Fig. 6.— The expected cumulative event rate for the KBS model of dark cloud occultations toward the Galactic bulge, LMC, and SMC when detection efficiencies are taken into account. Solid-lines represent halo clouds and the dashed-lines are for the disk cloud model.

In Figure 6 we plot the cumulative number of events expected for the KBS models. For disk clouds, the largest number of events per star is expected toward the Galactic bulge, while for a halo cloud population, the largest number of events per star is expected toward the SMC. In Figure 7, we plot the number of event detections expected when the stellar exposure time is considered. The total exposure for each target is the sum of the number of stars monitored in a field multiplied by the number of years it was monitored. If dark clouds following the KBS disk model contribute a third of disk mass density ($0.03M_{\odot}\text{pc}^{-3}$), then $\sim 100,000$ extinction events should have been discovered toward the Galactic bulge. Such a large number of events could not

have gone undetected in the data. For clouds in the KBS isothermal halo model, the maximum number of events would have been observed toward the Galactic bulge rather than the LMC or SMC. This is somewhat surprising, but is simply due to the fact that twice as many stars were observed toward the Galactic bulge as the LMC. For this model we should have detected $\sim 50,000$ events due to cloud extinctions.

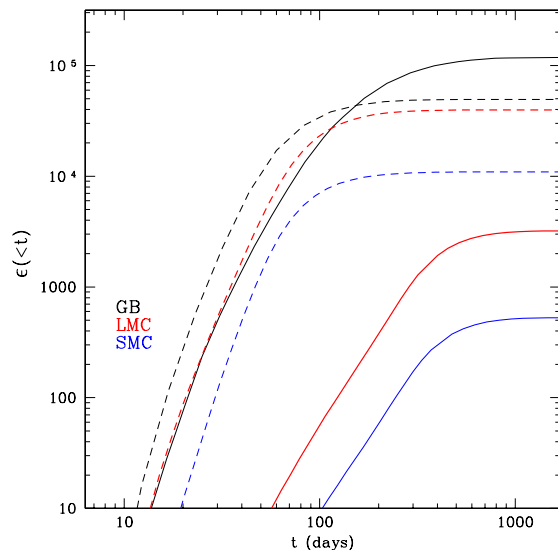


Fig. 7.— Cumulative number of cloud obscuration events expected with our analysis for the KBS models. The solid-lines present the halo cloud numbers and the dashed-lines the those for disk cloud models.

4.1. Efficiencies at Low Extinction

The number of events that we expect to detect is strongly dependent on the amount of extinction they cause. For extinctions greater than ~ 1 magnitude ($f \sim 0.08$) the obscuration event detection efficiency is approximately constant for all targets. To better quantify the number of obscuration events expected if the dark clouds have very small dust concentrations ($< 1\%$ that of molecular clouds), we performed a second set of detection efficiency simulations for extinctions

less than one magnitude.

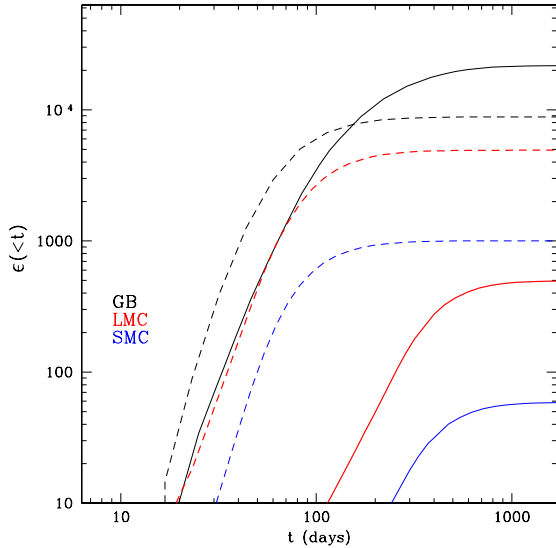


Fig. 8.— Cumulative number of cloud obscuration events expected for the KBS model when $A_V < 1$. The solid-lines present the halo cloud numbers and the dashed-lines those for disk cloud models.

In Figure 8 we present the number of low extinction clouds we expect to have detected in our analysis for the KBS models. In this case we still expect to have detected 20,000 events toward the bulge for disk clouds, or 9,000, if the clouds exist in an isothermal halo population. In Figure 9 we present the obscuration event detection efficiency as a function of the extinction caused by the cloud. The differences between the plotted detection efficiencies are mainly due to the different timescale distributions. The expected number of detections only falls to zero near the 0.2 magnitudes ($f \sim 0.2\%$) because of the cut we imposed in our selection. A non-standard extinction law would allow a larger amount of dust to go unnoticed. However, this would only change the result by a factor of ~ 2 .

The dark cloud occultation event timescale is proportional to the cloud size R and the event rate is proportional to $T^{-1}R^{-1}$. In this anal-

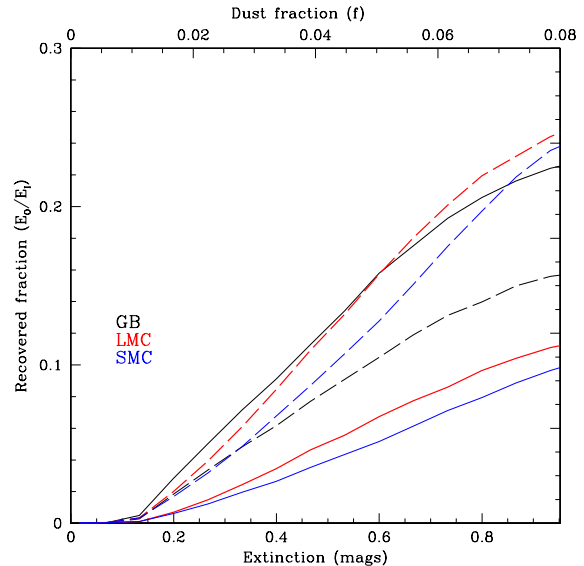


Fig. 9.— Obscuration event detection efficiency number for the KBS model when $A_V < 1$. The solid-lines present the halo cloud numbers and the dashed-lines those for disk cloud models.

ysis we have assumed the KBS model values ($T = 10\text{K}$, $M = 10^{-3}M_{\odot}$, and $R = 7\text{AU}$). For different dark cloud models the extinction events may appear as many short events or a small number of longer timescale events. For the adopted model, halo events peak in number at around 60 days, while for disk clouds the peak is near 100 days. From our efficiencies we should still have been able to detect obscuration events due to small clouds (with maximum ~ 10 days) or due to large clouds (with maximum number ~ 1000 days), because the cloud transit timescale distributions are broad. However, de Paolis (private communication) suggests that there are models in which large halo clouds would take 10 to 100 years to transit a background star. In such cases we still expect to have discovered a few clouds as they began to obscure stars (provided they produced more than 0.2 magnitudes of visual extinction). Our results do not show any trace of a low-mass dark cloud population.

5. DISCUSSION

In our analysis we have attempted to maximize our efficiency for detecting dark clouds obscuration events over a range of characteristic timescales and degrees extinctions. Our selection process should have allowed us to detect extinctions due to passing clouds even if they were non-spherical or had an internal dust distribution which was slightly anisotropic. However, we do not find any evidence for a population of dark clouds in either the disk or halo of our Galaxy. We can strongly rule out the existence of a population of dark ($A_V > 0.2$) clouds with the parameters of the KBS disk or halo model.

There are a number of possible ways a population of gaseous clouds may have been missed in this analysis. For instance, such clouds could have a very small dust content and therefore be almost completely transparent. In such cases gas lensing events can still occur. The mass and radius limits for possible clouds from Rafikov and Draine (2001) are approximately $10^{-4} \lesssim M \lesssim 2 \times 10^{-2} M_\odot$, $R < 200 \text{AU}$ (see their Figure 9). While our results seem to rule out the possibility that a population of dark clouds exist with masses from 10^{-4} to $10^{-2} M_\odot$. Together these results exclude the possibility of a dusty cloud population with a polytropic index of 1.5. Whether the proposed population of gaseous clouds are dusty is not certain. However, as we mentioned earlier, if the SCUBA sources of Lawrence (2001) are due to dark clouds, they must contain some dust to show continuous emission in the sub-mm band. The existence of dusty molecular clumps is also useful for explaining the EGRET background γ -ray emission results (Kalbera et al. 1999). It is possible that the dust in the clouds would not be readily observed from stellar obscuration events. For instance the dust may sediment to the core of the cloud (Wardle & Walker 1999). Alternatively, the clouds may be clumped into large dark clusters which exist only in regions far from the Galactic disk (Wasserman &

Salpeter 1994, de Paolis et al. 1995, 1998).

We would like to thank Kim Griest and Francesco de Paolis for encouraging us to perform this work. This work was performed under the auspices of the U.S. Department of Energy National Nuclear Security Administration by the University of California, Lawrence Livermore National Laboratory under contract W-7405-Eng-48.

REFERENCES

- Alcock, C., et al., 1997, *ApJ*, 491, 436
- Alcock, C., et al., 1999, *PASP*, 111, 1539
- Alcock, C., et al., 2000, *ApJ*, 542, 281
- Alcock, C., et al., 2001, *ApJ*, 562, 337
- Bond, I., et al., 2002, *A&A*, 333, 71
- Bennett, D.P., et al., 1993, *BAAS*, 25, 1402
- Binney, J., & Merrifield, M., 1998, *Galactic Astronomy*, Princeton Univ. Press, Princeton NJ
- Clayton, G., & Cardelli, J., 1988, *AJ*, 96, 695
- Cardelli, J.A., Clayton, G.C., & Mathis, J.S., 1989, *ApJ*, 345, 245
- de Paolis, F., Ingrassio, G., Jetzer, Ph., & Roncadelli, M., 1995, *A&A*, 295, 567
- de Paolis, F., Ingrassio, G., Jetzer, Ph., & Roncadelli, M., 1998, *ApJ*, 500, 59
- Derue, F., et al., 2000, *A&A*, 373, 126
- Fekel, F.C., Henry, G.W., & Eaton, J.A., 2002, *AJ*, 124, 1064
- Fiedler, T.L., et al., 1987, *Nature*, 326, 675
- Gerhard, O., & Silk, J., 1996, *ApJ*, 472, 34
- Henriksen, R.N., & Widrow, L.M., 1995, *ApJ*, 441, 70
- Kalberla, P.M.W., Schekinov, Yu.A., & Dettmar, R.J., 1999, *A&A*, 350, L9

Kamaya, H., & Silk, J., 2002, MNRAS, 335, L62

Keller, S.C., et al., 2002, AJ, 124, 2039

Kerins, E., Binney, J., & Silk, J., 2002, MNRAS, 332, L29 (KBS)

Kim, S-H., Martin, P.G., & Hendry, P.D., 1994, ApJ, 422, 164

Larson, K.A., et al. 2000, ApJ, 532, 1021

Lawrence, A., 2001, MNRAS, 323, 147

Murray, S.D., & Lin, D.N.C., 1990, ApJ, 363, 50

Rafikov, R.R., & Draine, B.T., 2001, ApJ, 547, 207

Pfenniger, D., & Combes, F., 1994, A&A, 285, 94

Sciama, D.W., 2000, MNRAS, 312, 33

Schechter, P., Mateo, M., & Saha, A., 1993, PASP, 103, 1342

Schlegel, D., Finkbeiner, D., & Davis, M., 1998, ApJ, 500, 553

Szomoru, A., & Guhathakurta, P., 1999, AJ, 117, 2226

Udalski, A., et al., 2000, Acta Astron., 50, 1

Udalski, A., 2002, astro-ph/0210367

Walker, M., & Wardle, M., 1998, ApJ, 498, L125

Wardle, M., & Walker M., 1999, ApJ, 527, L109

Wasserman, M., & Salpeter M., 1994, ApJ, 433, 670

This 2-column preprint was prepared with the AAS L^AT_EX macros v4.0.

TABLE 1
OBSERVATIONAL DATA.

Target	Obs	Stars	Fields	Exposure
Bulge	32856	3.32×10^7	94	1.71×10^8
LMC	45270	1.29×10^7	82	9.38×10^7
SMC	5975	2.48×10^6	6	1.83×10^7
Total	84101	4.85×10^7	182	2.83×10^8

NOTE.—Col. (5), the exposure is in star years.

TABLE 2
CANDIDATE OBSCURATION EVENTS.

Target	C_{Init}	C_{col}	C_{CA}	C_{var}	C_{HPM}	C_{RVR, χ_r^2}
Bulge	5284	372	217	128	83	10
LMC	6427	441	431	151	133	2
SMC	678	98	96	37	36	0

NOTE.—Candidates present toward the various targets after apply various selections: Col. (2), initial candidates. Col. (3), colour cuts are used to remove bright red variables. Col. (4), removing chromospherically-active stars. Col. (5), removing Be and semi-periodic variable stars. Col. (5), removing high proper motion stars. Col. (6), removing objects with fits $\chi_r^2 > 12$ or $R_{\text{VR}} < 2.8$.